Title	Study of Multilevel High-Resistance States in HfOx-Based Resistive Switching Random Access Memory by Impedance Spectroscopy
Author(s)	Li, H. K.; Chen, T. P.; Hu, S. G.; Liu, P.; Liu, Y.; Lee, P. S.; Wang, X. P.; Li, H. Y.; Lo, G. Q.
Citation	Li, H. K., Chen, T. P., Hu, S. G., Liu, P., Liu, Y., Lee, P. S., et al. (2015). Study of Multilevel High-Resistance States in HfOx-Based Resistive Switching Random Access Memory by Impedance Spectroscopy. IEEE Transactions on Electron Devices, 62(8), 2684-2688.
Date	2015
URL	http://hdl.handle.net/10220/39539
Rights	© 2015 IEEE. Personal use of this material is permitted. Permission from IEEE must be obtained for all other uses, in any current or future media, including reprinting/republishing this material for advertising or promotional purposes, creating new collective works, for resale or redistribution to servers or lists, or reuse of any copyrighted component of this work in other works. The published version is available at: [http://dx.doi.org/10.1109/TED.2015.2445339].

Study of Multilevel High Resistance States in HfO_x-Based Resistive Switching Random Access Memory by Impedance Spectroscopy

H. K. Li, T. P. Chen, S. G. Hu, P. Liu, Y. Liu, P. S. Lee, X. P. Wang, H. Y. Li, and G. Q. Lo

***Abstract*—Multilevel high resistance states are achieved in TiN/HfO_x/Pt resistive switching random access memory device by controlling the reset stop voltage. Impedance spectroscopy is used to study the multilevel high resistance states. It is shown that the high resistance states can be described with an equivalent circuit consisting of the major components R_s, R, and C corresponding to the series resistance of the TiON interfacial layer, the equivalent parallel resistance and capacitance of the leakage gap between the TiON layer and the residual conductive filament, respectively. These components show a strong dependence on the stop voltage, which can be explained in the framework of oxygen vacancy model and conductive filament concept. On the other hand, R is observed to decrease with *DC* bias, which can be attributed to the barrier lowering effect of the Coulombic trap well in the Poole-Frenkel emission model.**

***Index Terms*—Impedance spectroscopy, multilevel high resistance states, resistive switching random access memory (RRAM).**

I. INTRODUCTION

Resistive switching random access memory (RRAM) based on metal oxides like Al_2O_3, ZnO, NiO_x, TiO_2, and Cu_xO is promising in the application of next-generation non-volatile memory due to its simple structure, low power consumption, high read/write speed, and good reliability [1]-[7]. Recently, multilevel resistance states in RRAM devices have been demonstrated to increase the storage density of the RRAM device [8], [9]. Until now, most of the research works were focused on the performance improvement and reliability of the multibit storage, there are relatively few studies on the mechanism for the multilevel resistance states of RRAM device. In this work, impedance spectroscopy is employed to investigate multilevel high resistance states in TiN/HfO_x/Pt RRAM structure. Impedance spectroscopy is a powerful tool to examine the conduction properties of dielectric thin films, making it suitable for resistive switching property study [10], [11]. For the TiN/HfO_x/Pt RRAM structure used in this work, the multilevel high resistance states may be attributed to the different rupture degrees of the conductive filament, which is hard to be detected by the microscopic techniques such as transmission electron microscopy and scanning probe microscopy. However, through the analysis of the impedance measurement, we have been able to obtain information about the redox reaction relating to the change of TiON interfacial layer and rupture of the conductive filament for different high resistance states.

Manuscript received March 13, 2015; revised May 7, 2015; accepted June 6, 2015. This work was financially supported in part by MOE Tier 1 Grant under Grant RG 43/12 and in part by NTU-A*STAR Silicon Technologies Centre of Excellence under Grant M4070176.040. The work of Y. Liu was supported by NSFC under Grant 61274086. The review of this paper was arranged by Editor Y.-H. Shih.

H. K. Li is with the School of Electrical and Electronic Engineering, Nanyang Technological University, Singapore 639798, Singapore, and also with the Agency for Science, Technology and Research, Institute of Microelectronics, Singapore 117685, Singpore (e-mail: E120048@e.ntu.edu.sg).

T. P. Chen, S. G. Hu, and P. Liu are with the School of Electrical and Electronic Engineering, Nanyang Technological University, Singapore 639798, Singapore (e-mail: ECHENTP@ntu.edu.sg; HUSHAOGANG@ntu.edu.sg; LIUP0013@e.ntu.edu.sg).

Y. Liu is with State Key Laboratory of Electronic Thin Films and Integrated Devices, University of Electronic Science and Technology of China, Chengdu 610054, China (e-mail: yliu1975@uestc.edu.cn).

P. S. Lee is with the School of Materials Science and Engineering, Nanyang Technological University, Singapore 639798, Singapore (e-mail: pslee@ntu.edu.sg).

X. P. Wang, H. Y. Li and G. Q. Lo are with the Agency for Science, Technology and Research, Institute of Microelectronics, Singapore 117685, Singpore (e-mail: wangxin@ime.a-star.edu.sg; lihy@ime.a-star.edu.sg; logq@ime.a-star.edu.sg).

II. EXPERIMENT

The TiN/HfO_x/Pt RRAM structure was fabricated with the following sequence. Firstly, a 500 nm SiO_2 film was deposited on an 8-inch *p*-type Si wafer by plasma-enhanced chemical vapor deposition to prevent the leakage during the switching operation of the RRAM device. Then, 50 nm Pt/ 20 nm Ti layer was deposited by electron-beam evaporation to form the bottom electrode on the SiO_2 film. Subsequently, a 10 nm HfO_x layer was deposited by atomic layer deposition on the bottom electrode. Finally, a 100 nm TiN layer was deposited onto the HfO_x layer using DC sputtering and patterned to form the top electrode with the area of about 4 μm^2. A Keithley 4200 semiconductor characterization system was used to characterize the switching properties of the device. Impedance measurement of different high resistance states was carried out with an Agilent E4980A Precision LCR Meter in the frequency range of 20 Hz to 2 MHz with a 30 mV *AC* signal.

III. RESULTS AND DISCUSSIONS

Fig. 1 shows the typical bipolar resistive switching behavior

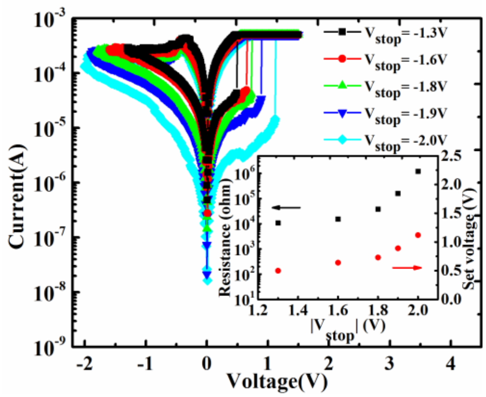

Fig. 1. Bipolar *I-V* curves of TiN/HfO_x/Pt RRAM device. Multilevel high resistance states can be achieved with different V_{stop}. The inset shows the values of the high resistance states created with different V_{stop} (read at 0.1 V) and the corresponding V_{set}.

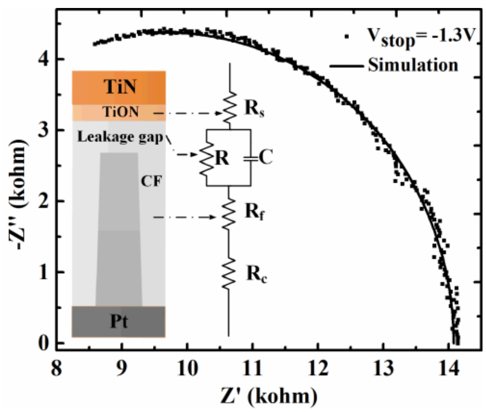

Fig. 2. Complex impedance spectra of the high resistance state obtained with the V_{stop} of -1.3V. The curve is the best fitting based on (2). The inset shows the schematic illustration of the conductive filament and the equivalent circuit for high resistance state.

of the TiN/HfO_x/Pt RRAM structure under different reset stop voltages (V_{stop}) ranging from -1.3 V to -2.0 V. Multilevel high resistance states can be achieved by varying V_{stop}. The inset of Fig. 1 shows the values of the high resistance states created with different V_{stop} (read at 0.1 V) and the corresponding set voltages (V_{set}). As observed in the inset of Fig. 1, the resistance of the device increases with $|V_{stop}|$. Based on the conductive filament model, when a positive voltage is applied to the TiN top electrode, the oxygen atoms inside the HfO_x layer will be knocked out of the lattice and become oxygen ions to react with the TiN electrode to form TiON [12]. The formation of TiON could result from the replacement of nitrogen by oxygen or defects that favor the incorporation of oxygen in the cation sub-lattice [13]. When the generated oxygen vacancies form a strong enough conductive filament to connect the top and bottom electrodes, the device will be set to a low resistance state. For the reset process, a negative voltage is applied to the top electrode, and the oxygen ions will move back to eliminate the oxygen vacancies, breaking the conductive filament; as a consequence, a leakage gap in the oxide is formed between the top electrode and the residual filament, as schematically illustrated in the inset of Fig. 2. When V_{stop} is of a larger magnitude, more oxygen ions will move back to the HfO_x layer to eliminate the oxygen vacancies, which will widen the gap between the top electrode and the residual conductive filament, and thus the resistance value will increase due to the gap widening [14]. In this case, the V_{set} during the following set process also increases with the magnitude of V_{stop}, as demonstrated in the inset of Fig. 1. It is because that a larger V_{set} is needed to rebuild the conductive filament for a wider leakage gap.

The above arguments could be verified with the impedance measurement. The complex impedance measurement is conducted after the reset process by applying a 30 mV small *AC* signal in the frequency range of 20 Hz to 2 MHz without *DC* bias. The scatter plot in Fig. 2 shows the complex impedance spectra of the high resistance state after reset operation with the V_{stop} of -1.3 V. The approximately semicircle shape of the Nyquist plots (-Z'' VS Z') indicates that the high resistance state can be modelled as a parallel connection of a resistor and a capacitor in series with some resistors, as shown in the inset of Fig. 2. The RRAM devices with other sizes (5×5 μm^2 and 8×8 μm^2) are also tested, and similar semicircle shapes of the Nyquist plots are observed (not shown here). This indicates that device size in the range has no influence on the equivalent circuit. The impedance of the equivalent circuit can be described with

$$Z = R_s + R_f + R_c + \frac{R}{1+\omega^2 R^2 C^2} - j\frac{\omega R^2 C}{1+\omega^2 R^2 C^2} \qquad (1)$$

where Z is the complex impedance, ω is the angular frequency, R_s, R_f and R_c are the equivalent series resistance for the TiON interfacial layer, residual conductive filament and measurement connections, respectively, and R and C are the equivalent parallel resistance and capacitance of the leakage gap, respectively. As discussed above, the redox reaction between the TiN electrode and the oxygen ions during the set process results in a TiON interfacial layer, which is more resistive than the pure TiN electrode. Though the series resistance should be the sum of the resistance of the TiON interfacial layer, residual filaments and measurement connections**,** the last two items can be neglected because of their much lower values [15]. Therefore, (1) can be rewritten as

$$Z = Z' + jZ'' = R_s + \frac{R}{1+\omega^2 R^2 C^2} + j(-\frac{\omega R^2 C}{1+\omega^2 R^2 C^2}) \qquad (2)$$

where Z' and Z'' are the real part and imaginary part of the complex impedance, respectively. The fitting with (2) to the measurement data is shown in Fig. 2. An excellent agreement between the fitting and measurement is achieved, which indicates that the equivalent circuit shown in the inset of Fig. 2 can well describe the electrical characteristic of the RRAM structure. The fitting yields the values of 5336 Ω, 8741 Ω and 9.81 pF for R_s, R and C, respectively. With the obtained R_s value, one may estimate the resistivity ρ of the TiON interfacial layer with $\rho = (A/t_{TiON})R_s$, where t_{TiON} is the thickness of the interfacial layer, and the device area A = 4 μm^2. Under the assumption that t_{TiON} is 5 nm [16], [17], the resistivity is estimated to be ~ 400 Ω·cm, which is within the reported resistivity range of TiON films [18].

To examine the behavior of different high resistance states, we conducted the complex impedance measurement after each

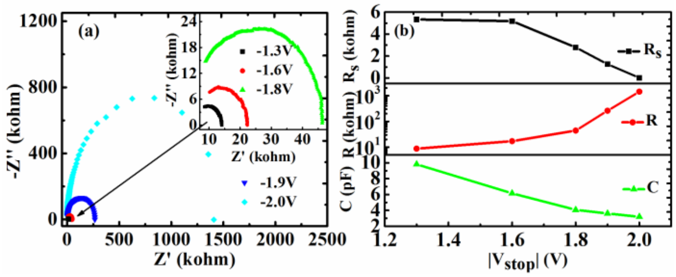

Fig. 3. (a) Complex impedance spectra of different high resistance states obtained with different $|V_{stop}|$. The inset in (a) shows the enlarged complex impedance spectra with the V_{stop} of -1.3 V, -1.6 V and -1.8 V. (b) The values of R_s, R and C as a function of $|V_{stop}|$.

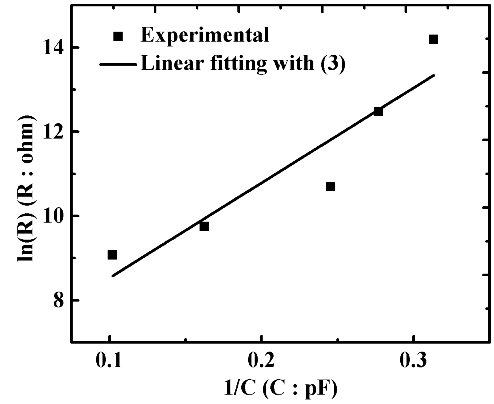

Fig. 4. *ln(R)* versus *1/C*.

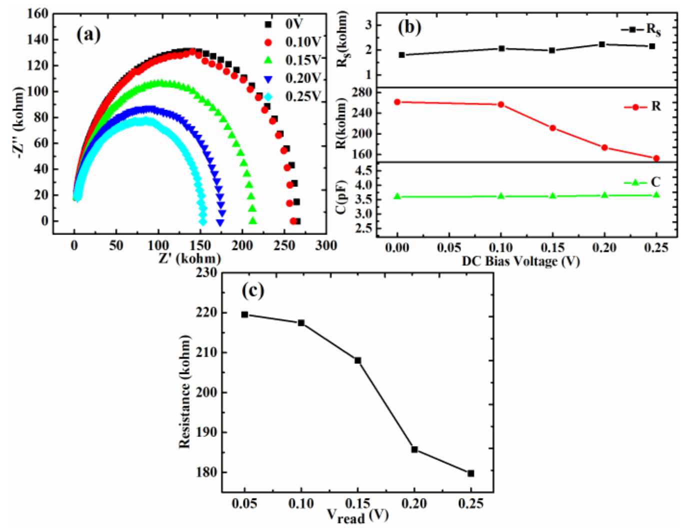

Fig. 5. (a) Complex impedance spectra of the high resistance state under different positive *DC* biases. (b) The values of R_s, R and C as a function of the *DC* bias. (c) The resistance value of the high resistance state as a function of V_{read}.

reset process at different V_{stop}, and the result is shown in Fig. 3(a). The Nyquist plots of all V_{stop} can be well fitted with (2), which indicates that all the high resistance states can be modelled with the equivalent circuit shown in the inset of Fig. 2. The values of the components in the equivalent circuit are shown in Fig. 3(b). The R_s value has an obvious decreasing trend when the V_{stop} changes from -1.3 V to -2.0 V. Since TiON is more resistive than pure TiN, the decrease of the R_s means more TiON is reduced to TiN for a larger $|V_{stop}|$. The parallel *RC* element represents the leakage gap between the top electrode and the residual conductive filament, and the modulation of the gap width is responsible for the changes in the *R* and *C* values. As shown in Fig. 3(b), the *R* value increases with the increase of $|V_{stop}|$, which means the width of the leakage gap gradually increases. It is reasonable to argue that the recombination of the oxygen vacancies with the oxygen ions supplied from the TiON layer or even the surrounding HfO_x layer is enhanced as the V_{stop} changes from -1.3 V to -2.0 V. It is worth noting that R_s and *R* have an opposite evolution tendency, while the change of the *DC* resistance, shown in the inset of Fig. 1, is consistent with the evolution of *R* because the *R* value is much larger than the R_s value. The capacitance of the *RC* element should be inversely proportional to the width of the leakage gap between the top electrode and the residual filament, being similar to the situation of a parallel plate capacitor; thus the decrease in the *C* value with $|V_{stop}|$ suggests that a larger $|V_{stop}|$ results in a wider leakage gap. Therefore, both dependence of *R* and *C* on $|V_{stop}|$ suggest that the leakage gap width increases with $|V_{stop}|$, which explains the increase of the *DC* resistance with $|V_{stop}|$ as shown in the inset of Fig. 1.

C can be described with $C = \varepsilon_r\varepsilon_0 A/t_{ox}$, where ε_0 is the permittivity in vacuum, and ε_r and t_{ox} are the dielectric constant and thickness of the leakage gap, respectively; and *R* can be assumed to be $R = R_0 exp(\alpha t_{ox})$, where R_0 and α are two constants as it has been suggested by Monte Carlo simulation that *R* has an exponential dependence on t_{ox} [19], [20]. Under the above assumptions, one may find the simple relationship between *R* and *C* as follows

$$\ln R = \ln R_o + \frac{\varepsilon_o \varepsilon_r \alpha A}{C} \tag{3}$$

The linear relationship between *ln(R)* and *1/C* predicted by (3) roughly agrees with the experimental result, as shown in Fig. 4.

To examine the influence of *DC* bias on the complex impedance measurement, a positive voltage ranging from 0 V to 0.25 V was superimposed to the *AC* signal during the impedance measurement, and the complex impedance spectra of the high resistance state under different positive *DC* biases are shown in Fig. 5(a). The semicircle shape of all the Nyquist plots indicates that the *DC* bias has little influence on the equivalent circuit of the high resistance state. The values of R_s, *R* and *C* obtained from the fitting as a function of the *DC* bias are shown in Fig. 5(b). Only the *R* has an obvious decreasing trend with the increase of *DC* bias. The little change of both R_s and *C* indicates that the redox reaction at the TiN/HfO_x interface is not significant under the influence of a small positive *DC* bias and the leakage gap should change little or remain unchanged. Therefore the change of the *R* value cannot origin from the leakage gap modulation effect. Previous studies on the current transport in HfO_x-based RRAM device show that Poole-Frenkel emission model can well describe the conduction of the high resistance state; and the oxygen vacancies inside the HfO_x layer could act as the Coulombic traps in the Poole-Frenkel emission model [21], [22]. When a bias is applied to the switching layer, one side of the barrier height of the Coulombic traps will be reduced, the probability for the electrons escaping from the trap well by thermal emission increases, thus the R value will decrease with increasing DC bias [23]. The decrease of R with DC bias is indeed observed in Fig. 5(b). This is also consistent with the experimental result shown in Fig. 5(c) that the DC resistance of the high resistance state decreases with the read voltage (V_{read}).

IV. CONCLUSION

In conclusion, impedance spectroscopy is a useful technique to study multilevel high resistance states in HfO_x-based RRAM device. The analysis of complex impedance suggests that the redox reaction at the TiN/HfO_x interface and the modulation of the leakage gap should be responsible for the changes in the parameters of the equivalent circuit of the RRAM device. The leakage gap widening effect is shown to be the main reason for the higher resistance value associated with a larger $|V_{stop}|$. Both R_s and C show little change with DC bias; however, R decreases with the DC bias, which can be attributed to the barrier lowering effect of the Coulombic trap well in the Poole-Frenkel emission model.

REFERENCES

[1] H. Y. Jeong, J. Y. Lee, and S.-Y. Choi, "Interface-Engineered Amorphous TiO_2-Based Resistive Memory Devices," *Adv. Funct. Mater.*, vol. 20, no. 22, pp. 3912–3917, Nov. 2010.

[2] W. Zhu, T. P. Chen, Z. Liu, M. Yang, Y. Liu, and S. Fung, "Resistive switching in aluminum/anodized aluminum film structure without forming process," *J. Appl. Phys.*, vol. 106, no. 9, p. 093706, 2009.

[3] F. Nardi, D. Deleruyelle, S. Spiga, C. Muller, B. Bouteille, and D. Ielmini, "Switching of nanosized filaments in NiO by conductive atomic force microscopy," *J. Appl. Phys.*, vol. 112, no. 6, p. 064310, 2012.

[4] B. J. Choi, D. S. Jeong, S. K. Kim, C. Rohde, S. Choi, J. H. Oh, H. J. Kim, C. S. Hwang, K. Szot, R. Waser, B. Reichenberg, and S. Tiedke, "Resistive switching mechanism of TiO_2 thin films grown by atomic-layer deposition," *J. Appl. Phys.*, vol. 98, no. 3, p. 033715, 2005.

[5] C.-Y. Liu, Y.-H. Huang, J.-Y. Ho, and C.-C. Huang, "Retention mechanism of Cu-doped SiO_2-based resistive memory," *J. Phys. D. Appl. Phys.*, vol. 44, no. 20, p. 205103, May 2011.

[6] C.-Y. Lin, D.-Y. Lee, S.-Y. Wang, C.-C. Lin, and T.-Y. Tseng, "Effect of thermal treatment on resistive switching characteristics in Pt/Ti/Al_2O_3/Pt devices," *Surf. Coatings Technol.*, vol. 203, no. 5–7, pp. 628–631, Dec. 2008.

[7] C.-Y. Lin, C.-Y. Wu, C.-Y. Wu, C. Hu, and T.-Y. Tseng, "Bistable Resistive Switching in Al_2O_3 Memory Thin Films," *J. Electrochem. Soc.*, vol. 154, no. 9, p. G189, 2007.

[8] Y. Wang, Q. Liu, S. B. Long, W. Wang, Q. Wang, M. H. Zhang, S. Zhang, Y. T. Li, Q. Y. Zuo, J. H. Yang, and M. Liu, "Investigation of resistive switching in Cu-doped HfO_2 thin film for multilevel non-volatile memory applications.," *Nanotechnology*, vol. 21, no. 4, p. 045202, Jan. 2010.

[9] R. Q. Chen, W. Hu, L. L. Zou, W. Xie, B. J. Li, and D. H. Bao, "Multilevel resistive switching effect in sillenite structure $Bi_{12}TiO_{20}$ thin films," *Appl. Phys. Lett.*, vol. 104, no. 24, p. 242111, Jun. 2014.

[10] J. T. S. Irvine, D. C. Sinclair, and A. R. West, "Electroceramics: Characterization by Impedance Spectroscopy," *Adv. Mater.*, vol. 2, no. 3, pp. 132–138, Mar. 1990.

[11] X. L. Jiang, Y. G. Zhao, Y. S. Chen, D. Li, Y. X. Luo, D. Y. Zhao, Z. Sun, J. R. Sun, and H. W. Zhao, "Characteristics of different types of filaments in resistive switching memories investigated by complex impedance spectroscopy," *Appl. Phys. Lett.*, vol. 102, no. 25, p. 253507, 2013.

[12] Z. Fang, H. Y. Yu, W. J. Liu, Z. R. Wang, X. A. Tran, B. Gao, and J. F. Kang, "Temperature Instability of Resistive Switching on HfO_x-Based RRAM Devices," *IEEE Electron Device Lett.*, vol. 31, no. 5, pp. 476–478, 2010.

[13] T. H. Fang and K. T. Wu, "Local oxidation characteristics on titanium nitride film by electrochemical nanolithography with carbon nanotube tip," *Electrochem. commun.*, vol. 8, no. 1, pp. 173–178, 2006.

[14] F. Nardi, S. Larentis, S. Balatti, D. C. Gilmer, and D. Ielmini, "Resistive Switching by Voltage-Driven Ion Migration in Bipolar RRAM — Part I : Experimental Study," *IEEE Trans. Electron Devices.*, vol. 59, no. 9, pp. 2461–2467, 2012.

[15] Q. J. Li, K. Ali, S. Iulia, P. Christos, H. Xu, and P. Themistoklis, "Memory Impedance in TiO_2 based Metal-Insulator-Metal Devices.," *Sci. Rep.*, vol. 4, p. 4522, Jan. 2014.

[16] H. Z. Zhang, D. S. Ang, C. J. Gu, K. S. Yew, X. P. Wang, and G. Q. Lo, "Role of interfacial layer on complementary resistive switching in the TiN/HfO_x/TiN resistive memory device," *Appl. Phys. Lett.*, vol. 105, no. 22, p. 222106, Dec. 2014.

[17] S. M. Yu, H.-Y. Chen, B. Gao, J. Kang, and H.-S. P. Wong, "HfO_x-Based Vertical Resistive Switching Random Access Memory Suitable for Bit-Cost-Effective Three-Dimensional Cross-Point Architecture.," *ACS Nano*, vol. 7, no. 3, pp. 2320–2325, Feb. 2013.

[18] F. L. Chen, S.-W. Wang, L. M. Yu, X. S. Chen, and W. Lu, "Control of optical properties of TiN_xO_y films and application for high performance solar selective absorbing coatings," *Opt. Mater. Express*, vol. 4, no. 9, p. 1833, 2014.

[19] X. M. Guan, S. M. Yu, and H. P. Wong, "On the Switching Parameter Variation of Metal-Oxide RRAM — Part I : Physical Modeling and Simulation Methodology," *IEEE Trans. Electron Devices.*, vol. 59, no. 4, pp. 1172–1182, 2012.

[20] S. M. Yu, X. M. Guan, and H. P. Wong, "On the Switching Parameter Variation of Metal Oxide RRAM — Part II : Model Corroboration and Device Design Strategy," *IEEE Trans. Electron Devices.*, vol. 59, no. 4, pp. 1183–1188, 2012.

[21] B. Long, Y. B. Li, S. Mandal, R. Jha, and K. Leedy, "Switching dynamics and charge transport studies of resistive random access memory devices," *Appl. Phys. Lett.*, vol. 101, no. 11, p. 113503, 2012.

[22] C. Walczyk, C. Wenger, R. Sohal, M. Lukosius, a. Fox, J. Dąbrowski, D. Wolansky, B. Tillack, H.-J. Müssig, and T. Schroeder, "Pulse-induced low-power resistive switching in HfO_2 metal-insulator-metal diodes for nonvolatile memory applications," *J. Appl. Phys.*, vol. 105, no. 11, p. 114103, 2009.

[23] M. Ieda, G. Sawa, and S. Kato, "A Consideration of Poole-Frenkel Effect on Electric Conduction in Insulators," *J. Appl. Phys.*, vol. 42, no. 10, p. 3737, 1971.

H. K. Li received the B.S. and M.S. degrees in microelectronics and solid state electronics from Huazhong University of Science and Technology, Wuhan, China, in 2009 and 2012, respectively.

He is currently pursuing the Ph.D. degree at Nanyang Technological University, Singapore.

T. P. Chen received the Ph.D. degree from The University of Hong Kong in 1994.

He is currently an Associate Professor with the School of Electrical and Electronic Engineering, Nanyang Technological University, Singapore.

S. G. Hu received the B.S. degree from University of Electronic Science and Technology of China (UESTC) in 2008.

He is currently pursuing the Ph.D. degree in UESTC.

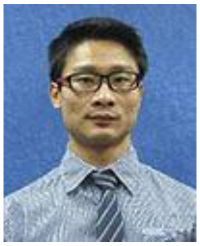

P. Liu received the B.S. degree from the Nanyang Technological University (NTU) of Electrical and Electronic Engineering, Singapore.

He is currently pursuing the Ph.D. degree at NTU.

Y. Liu received the Ph.D. degree from Nanyang Technological University, Singapore, in 2005.

He joined the University of Electronic Science and Technology of China, Chengdu, China, where he has been a Full Professor since 2008.

P. S. Lee received the Ph.D. degree from National University of Singapore (NUS), Singapore, in 2001.

She is currently an Associate Professor with the School of Materials Science and Engineering, Nanyang Technological University, Singapore.

X. P. Wang received the B.Eng. and M.Eng. degrees from Tsinghua University, Beijing, China, and Ph.D. degree from National University of Singapore, Singapore, in 1999, 2002, and 2007, respectively.

He is currently a Scientist with the Institute of Microelectronics, Agency for Science, Technology and Research, Singapore.

H. Y. Li received the Ph.D. degree in semiconductor physics and devices from the Changchun Institute of Physics, Chinese Academy of Science, Changchun, China, in 1999.

She is currently a Scientist with the Institute of Microelectronics, Agency for Science, Technology and Research, Singapore.

G. Q. Lo received the M.S. and Ph.D. degrees in electrical and computer engineering from the University of Texas at Austin, Austin, in 1989 and 1992, respectively.

Since 2004, he has been with the Institute of Microelectronics (IME), Agency for Science, Technology and Research, Singapore. He is currently the Laboratory Director for IME's Semiconductor Process Technology and the Program Director of Nanoelectronics and Photonics program.